NeuroImage: Clinical 33 (2022) 102917

Contents lists available at ScienceDirect

NeuroImage: Clinical

journal homepage: www.elsevier.com/locate/ynicl

Alterations of dynamic redundancy of functional brain subnetworks in Alzheimer's disease and major depression disorders

Maryam Ghanbari, Mayssa Soussia, Weixiong Jiang, Dongming Wei [1], Pew-Thian Yap, Dinggang Shen [2,3], Han Zhang [2,*]

Department of Radiology and BRIC, University of North Carolina at Chapel Hill, Chapel Hill, NC 27599, USA

ARTICLE INFO

Keywords:
Dynamic functional connectivity
Graph theory
Complex network
Resilience
Alzheimer's disease
Depression

ABSTRACT

The human brain is not only efficiently but also "redundantly" connected. The redundancy design could help the brain maintain resilience to disease attacks. This paper explores subnetwork-level redundancy dynamics and the potential of such metrics in disease studies. As such, we looked into specific functional subnetworks, including those associated with high-level functions. We investigated how the subnetwork redundancy dynamics change along with Alzheimer's disease (AD) progression and with major depressive disorder (MDD), two major disorders that could share similar subnetwork alterations. We found an increased dynamic redundancy of the subcortical-cerebellum subnetwork and its connections to other high-order subnetworks in the mild cognitive impairment (MCI) and AD compared to the normal control (NC). With gained spatial specificity, we found such a redundancy index was sensitive to disease symptoms and could act as a protective mechanism to prevent the collapse of the brain network and functions. The dynamic redundancy of the medial frontal subnetwork and its connections to the frontoparietal subnetwork was also found decreased in MDD compared to NC. The spatial specificity of the redundancy dynamics changes may provide essential knowledge for a better understanding of shared neural substrates in AD and MDD.

1. Introduction

Resting-state fMRI (rs-fMRI)-derived functional connectivity (FC) reflects information exchanges and coordination among different brain regions, resulting in large-scale brain functional networks (Sporns, 2013). It has been suggested that brain FC is time-varying and non-stationary, possibly reflecting adaptive control and attention fluctuations during resting state (Chang & Glover, 2010). Such a dynamic connectome (a.k.a., "chronnectome") could be altered by many brain diseases and mental disorders (Marusak, et al., 2017). Many studies have used graph theory as a powerful tool to investigate the brain network's efficiency and how brain diseases alter it (Xuan, et al., 2017). Among many efficiency metrics, the characteristic path length (Liu, et al., 2017) (i.e., the shortest paths) and its derivatives (e.g., assortativity and resilience), including the small-worldness (Newman, 2006; Ravasz & Barabási, 2003; Achard, et al., 2006) have been extensively investigated. These metrics, including their dynamics, have performed well on analyzing sparse brain networks that often include a few strong connections. On the contrary, in denser networks where weaker connections are also included, redundancy could become a *dominant* property.

However, characterizing brain network's redundancy and its changes over a short time (i.e., redundancy dynamics) is largely neglected in the previous brain research. For instance, one may calculate the number of *independent paths* in the brain network as a redundancy measurement to quantify the robustness of the network under possible attacks that could occur brain wide. While such a redundancy analysis on many natural networks has been extensively conducted (Corson, 2010; Härkegård & Glad, 2005), brain network studies are still very scarce. A magnetoencephalography (MEG)-based FC study (Di Lanzo, et al., 2012) used various redundancy metrics at each frequency band and revealed that the functional brain network was more redundant than a random network. In the study, the average number of alternative

* Corresponding author.
E-mail address: zhanghan2@shanghaitech.edu.cn (H. Zhang).
[1] Present address: School of Biomedical Engineering, Shanghai Jiao Tong University, Shanghai, 200030, China.
[2] Present address: School of Biomedical Engineering, ShanghaiTech University, Shanghai, 201210, China.
[3] Present address: Shanghai United Imaging Intelligence Co., Ltd. Shanghai, China.

https://doi.org/10.1016/j.nicl.2021.102917
Received 2 August 2021; Received in revised form 5 December 2021; Accepted 13 December 2021
Available online 14 December 2021

paths was used as the redundancy metric. In another electroencephalogram (EEG) study on spinal cord injured patients, a redundancy measurement of the entire FC network was used but showed no significant changes compared to healthy subjects (Fallani, et al., 2011). It was also found that education level could strengthen the redundancy of diffusion MRI-derived brain structural connectivity network of Alzheimer's disease (AD) patients compared to normal controls (NC) (Yoo, et al., 2015). A major depressive disorder (MDD) study showed a reduction in the brain network's redundancy in MDD patients compared to NC during stimulus processing (Leistritz, et al., 2013).

The major drawback in the previous brain network redundancy studies is that none of them investigated redundancy in the dynamic brain functional network that may reflect the higher functional significance of the brain network redundancy than the static one. Whether the FC dynamics also lead to dynamics in the network redundancy, and whether such alterations can be sufficiently sensitive to brain diseases so that it could be utilized for brain disease studies, remains unknown. As such, in our recent works, we proposed to measure the dynamic redundancy of the whole brain network (Ghanbari, et al., 2020; Ghanbari, et al., 2021). We defined a new brain state that every pair of brain regions were connected through at least two independent paths (with no node shared) as a *redundant state*, and calculated its dynamics as one of the major redundancy metrics. We found an increased chance of the whole-brain redundancy along time in the mild cognitive impairment subjects (MCI), an early stage of AD, compared to the NC (Ghanbari, et al., 2020, Ghanbari, et al., 2021). We further designed an individualized early AD detection method based on a decision tree with the dynamic redundancy metrics as features, which reached an accuracy of 90% in the classification between MCI and NC (Ghanbari, et al., 2020). While this method seems promising, it lacks spatial specification, as all the redundancy metrics were defined on the *entire* network without knowing which specific subnetwork has redundancy changes. Disease studies may be more interested in where such redundancy changes take place. Meanwhile, by focusing on more dynamic redundancy features, one could increase the sensitivity in group difference detection, whereas the whole-brain metric could have reduced sensitivity due to the average effect. It could be possible that different brain subnetworks, due to their specific cognitive roles (Smith, et al., 2009), may be affected differently and show different dynamic redundancy changes. Without the spatial resolution, whole-brain avaraged redundancy may not reveal such subnetwork-level changes.

Cognitive dysfunction is prevalent in neurological and psychiatric disorders. Two typical disorders, AD and MDD, could develop cognitive dysfunction at certain stage of the diseases (Sierksma, et al., 2010) and may share broad similarities in brain structural changes such as hippocampal volume loss (Sampath, et al., 2017) as well as brain subnetwork disconnection, especially within and among a set of cognitive function-related subnetworks (Menon 2011). In this study, we performed subnetwork-level dynamic redundancy analysis on two disease cohorts (AD and MDD) and investigated the redundancy dynamics of each cognitive function-related brain functional subnetwork and the redundancy dynamics of the inter-subnetwork connections. We hypothesized that the two disease cohorts (AD and MDD) may share similar cognitive dysfunction symptoms and thus could have similar overlapping underlying neural features as revealed by the subnetwork-level redundancy dynamics.

2. Materials and methods

2.1. Datasets

In *Study 1*, we used the Alzheimer's Disease Neuroimaging Initiative (ADNI) dataset. A participant with or without subjective memory complaints, verified by a study partner, with Mini-Mental State Exam score between 24 and 30 inclusive, and also Clinical Dementia Rating equals 0 and Memory Box score 0, belongs to NCs. While participants were diagnosed as MCIs if they expressed a subjective memory concern as reported by the participant or recalled by study partner or clinician with Mini-Mental State Exam (MMSE) score between 24 and 30 inclusive, and also Clinical Dementia Rating equals 0.5 and Memory Box score at least 0.5. However, participants were diagnosed as AD if they expressed a subjective memory concern as reported by the participant or recalled by study partner or clinician and Mini-Mental State Exam score between 20 and 24 inclusive with Clinical Dementia Rating equals 0.5 or 1.0 (http://adni.loni.usc.edu/). The 7-min rs-fMRI data (140 volumes, repetition time = 3 s, slice thickness = 3.5 preferred, 4.5 mm maximum, flip angle = 80°, matrix size = 64 × 64) was preprocessed using AFNI (Cox, 1996) according to a standard pipeline (Yan & Zang, 2010). Specifically, the first ten volumes are discarded, followed by a rigid-body head motion correction and a nonlinear spatial registration to the Montreal Neurological Institutes (MNI) space. The subjects with large head motion (i.e., larger than 2 mm or 2°) and those who had more than 2.5 min rs-fMRI data with large (greater than0.5 mm) frame-wise displacement were excluded (Chen, et al., 2017). A total of 6 ADs, 3 MCIs and 17 NCs were excluded due to excessive head motion. Mean rs-fMRI time series of each brain region defined by Shen's 268-region atlas (Shen, et al., 2013), was band-pass filtered (0.015–0.15 Hz), before it was further processed to reduce artifacts by regression analysis (nuisance regressors included head motion parameters according to the "Friston-24" model, the mean rs-fMRI signal in the white matter, and that in the cerebrospinal fluid). A total of 49 NC (26 males and 23 females, age 73.1 ± 6.5, MMSE 29.1 ± 1.0), 49 MCI (26 males and 23 females, age 74.3 ± 9.8, MMSE 27.9 ± 1.6), and 49 AD (26 males and 23 females, age 73.3 ± 8.5, MMSE 23.1 ± 2.5) subjects were selected from the ADNIGo and the ADNI2. Specifically, we found that 49 AD subjects had baseline fMRI data, while the NC and MCI groups had more subjects than the AD group. Therefore, we selected the baseline data (or the follow-up data that was closest to the baseline data, if the baseline data had excessive head motion) NC and MCI subjects at the similar age (±2 years) and of the same gender as each of the AD subjects to make sure a good match of subjects among the three groups. Due to the limited sample size (N = 49) of ADs, we selected the same amount (N = 49) of NC and MCI subjects, respectively, to make sure as many matched data as possible were used. The three groups were age-matched (p = 0.752, one-way analysis of variance (ANOVA)) and gender-matched.

In *Study 2*, we used a dataset collected from our collaborative hospital, the First Affiliated Hospital of Guangzhou University of Chinese Medicine, Guangdong, China from September 2015 to June 2018. After an initial screening utilizing the 17-item Hamilton Rating Scale for Depression (HDRS-17) with a total score larger than 18 (Hamilton, 1967), two expert psychologists (with at least ten years experience) separately diagnosed the MDD patients according to the Diagnostic and Statistical Manual (DSM-5, American Psychiatric Association, 2013). Only if both psychologists diagnosed a patient as MDD, then that subject was recruited. The inclusion criteria of MDD are as follows: (a) aged between 18 and 55 years old, (b) right-handed native Chinese speaker, (c) firstly diagnosed with MDD and had no history of any neurological illness or any other forms of psychiatric disorders, and (d) head motion smaller than 2 mm of translation or 2° of rotation in any direction during the rs-fMRI scan. Exclusion criteria included (a) a history of significant medical illness (15 participants were excluded), (b) alcohol abuse (a total score ≥ 8 in Alcohol Use Disorders Identification Test (Saunders, et al., 1993)), (0 participants were excluded), and (c) contraindications to MRI scan, (6 participants were excluded). The rs-fMRI and 3D T1-weighted images (3D-T1WI) in the MDD dataset had the following parameters: repetition time / echo time = 2,000/30 ms, flip angle = 90°, matrix size = 64 × 64, field of view (FOV) = 240 mm × 240 mm, slices number = 33, slice thickness = 4.0 mm, scanning time = 8′20′′ (250 volumes) for the rs-fMRI, and TR/TE = 10.4/4.3 ms, flip angle = 15°, slice thickness = 1.0 mm, slice gap = 0 mm, matrix size = 256 × 256, FOV = 256 mm × 256 mm, and slices number = 156 for the 3D-T1WI. The image preprocessing was performed using SPM12 (www.fil.ion.ucl.

ac.uk/spm) and Data Processing Assistant for Resting-State fMRI (DPARSF) version 2.3 (http://rfmri.org/DPARSF). For each subject, the first ten volumes were removed. The remaining images were corrected for slice acquisition timing and head motion. The 3D-T1WI was used to guide rs-fMRI registration using the unified segment and Diffeomorphic Anatomical Registration through Exponentiated Lie Algebra (DARTEL) in SPM12. The rs-fMRI data were smoothed with a 6-mm full-width-at-half-maximum Gaussian kernel, and further denoised by regressing out several nuisance signals, including the Friston-24 head motion parameters and signals from cerebrospinal fluid and white matter, before linear detrending and temporal band-pass filtering (0.01–0.08 Hz).The same data was previously used in another study (Li, et al., 2020), which included 66 NC (35 males and 31 females, age 29.3 ± 10.1) and 66 MDD (41 males and 25 females, age 29.5 ± 9.9). The two groups were age ($p = 0.931$, two-sample t-test) and gender-matched ($p = 0.379$, chi-square test). The MDD group had a Hamilton Depression Rating Scale (HAMD, a measurement of disease severity) of 22.3 ± 3.6 and a disease duration of 9.1 ± 1.9 months. This study was conducted in accordance with the Declaration of Helsinki. All participants provided written informed consent and the study was approved by the local ethics committee.

2.2. Subnetwork definitions

We adopted a widely used functional parcellation atlas (Shen, et al., 2013). The 268 brain regions had been clustered using a group-wise spectral clustering algorithm, generating eight functional subnetworks. They were further identified and named as the medial frontal, frontoparietal, default mode, subcortical-cerebellum, motor, visual I, visual II, and visual association networks. In this study, we evaluated the dynamic redundancy of four subnetworks in the AD study, including the medial frontal, frontoparietal, default mode, and subcortical-cerebellum networks, since many studies have shown alterations in these four subnetworks due to AD (Cui, et al., 2018; Xue et al., 2019). In the MDD study, since the previous studies indicated that the first three subnetworks could be involved (Bludau, et al., 2016; Yan, et al., 2019); we only focused on the first three subnetworks. The four subnetworks were visualized in Fig. 1.

2.3. Network redundancy

Similar to our previous studies (Ghanbari, et al., 2020; Ghanbari, et al., 2021), we used a set of well-adopted connectedness metrics in the field of graph theory. Specifically, a network G with a node set V (G) and an edge set E(G) is connected if there is a path between every pair of its nodes. A connected network G is called 2-connected if, for every two nodes ×, y ∈ V (G), there are at least two "independent" paths between × and y that do not share any node(s) except x and y themselves. Fig. 2A depicts a connected graph but it is not 2-connected because of the existence of a shared node. Fig. 2B shows a 2-connected graph because there are at least two independent paths for every pair of nodes. Therefore, this is a redundant network that is resilient to any attacks (the graph is still connected after removing any node or link). Please note that such a redundancy definition is quite strict as it defines the redundancy of the entire network. While previous graph theory analysis also measured brain network's resiliency by calculating the reduction of network efficiency after targeted removal of high centrality nodes or after random removal certain number of nodes (Joyce, et al., 2013); these methods were still efficiency-based and not as strict as our method.

2.4. Dynamic network redundancy

We calculated dynamic binary brain functional networks and quantified dynamic network redundancy on each selected subnetwork and inter-subnetwork connections between each pair of the subnetworks. First, for each subnetwork (Fig. 3A) of each subject in each group (we did the same for the graph consisting of inter-subnetwork connections between each pair of the subnetworks), we generated T sliding windows to calculate the dynamic FC based on pairwise Pearson's correlation (Fig. 3B). The window length was set to 60 s (20 volumes for the AD dataset and 30 volumes for the MDD dataset), and the step size was set to one volume (3 s for the AD dataset and 2 s for the MDD dataset). Second, for every window t, $1 \leq t \leq T$, we applied D density levels to generate D binary networks (Fig. 3C). Third, we defined redundancy states (either state #1 or state #2) for every time window (Fig. 3D). Let $\mathbf{r}:=\{r_t\}$ ($1 \leq t \leq T$) be the redundancy state vector where $r_t = 1$ if the minimally connected network in t is not 2-connected and $r_t = 2$, otherwise. Of note, the density level to have the minimal 2-connected network is higher than or equal to the density level that the network is minimally connected. This is the reason that we defined redundancy states as whether the density level of the minimal 2-connected network is the same as the density level of the minimal connected network. In other words, we set the redundancy index for a network to "2″ if the minimal 2-connected and the minimal connected networks have the same density level and we "1" if the minimal connected network is not 2-connected. For example, $\mathbf{r} = \{1, 2, 2, \ldots, 1\}$ describes redundancy state changes in Fig. 3D. Finally, we quantified the dynamic redundancy by calculating the occurrence frequency of the state #2 during the entire scan time from **r**, generating a "*redundancy index*" for a subnetwork or a pair of subnetworks. This index measures the probability (between 0 and 1) that a network is also 2-connected when it is minimally connected (with the lowest density to ensure its connectedness) through time. Thus, the more the redundancy index is, the more frequent back-up paths exist for *every* pair of the network. In other words, the network with a higher redundancy index is more likely to have an optimized topology along time that makes it robust to any attacks. We obtained ten redundancy indices for each subject in the AD study, four for each subnetwork, and six for all pairs of the subnetworks. In the MDD study, six redundancy indices were obtained for every subject (since three subnetworks were

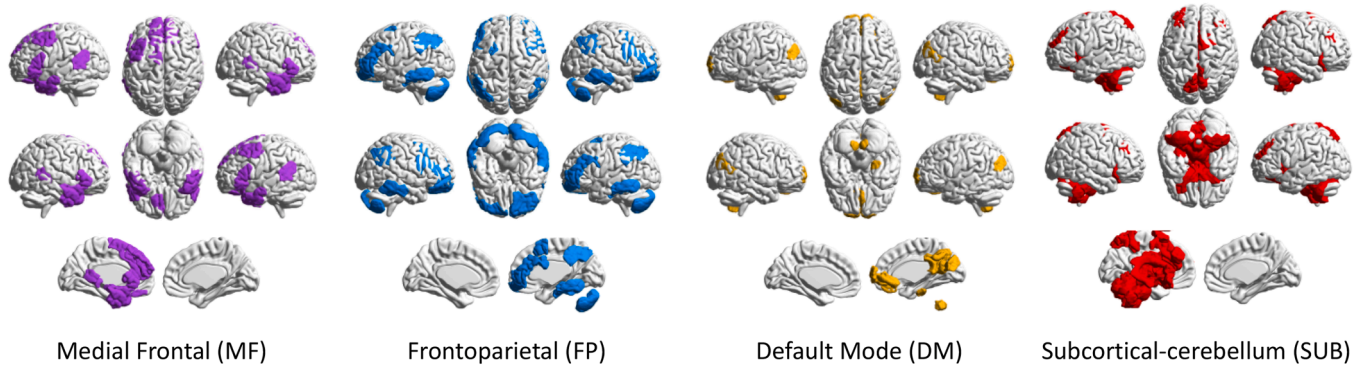

Fig. 1. Visualization of the four functional subnetworks derived from the Shen 268 atlas. From left to right: the medial frontal (MF), frontoparietal (FP), default mode (DM), and subcortical-cerebellum (SUB) subnetworks.

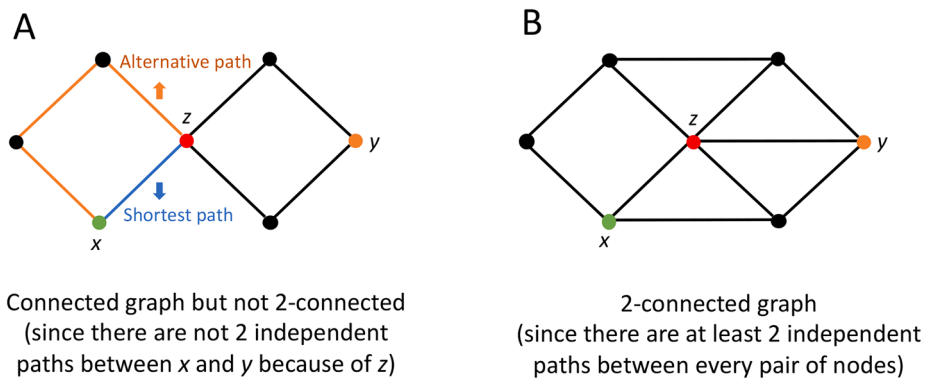

Fig. 2. Examples of a connected network that is not 2-connected (A) and a 2-connected network (B).

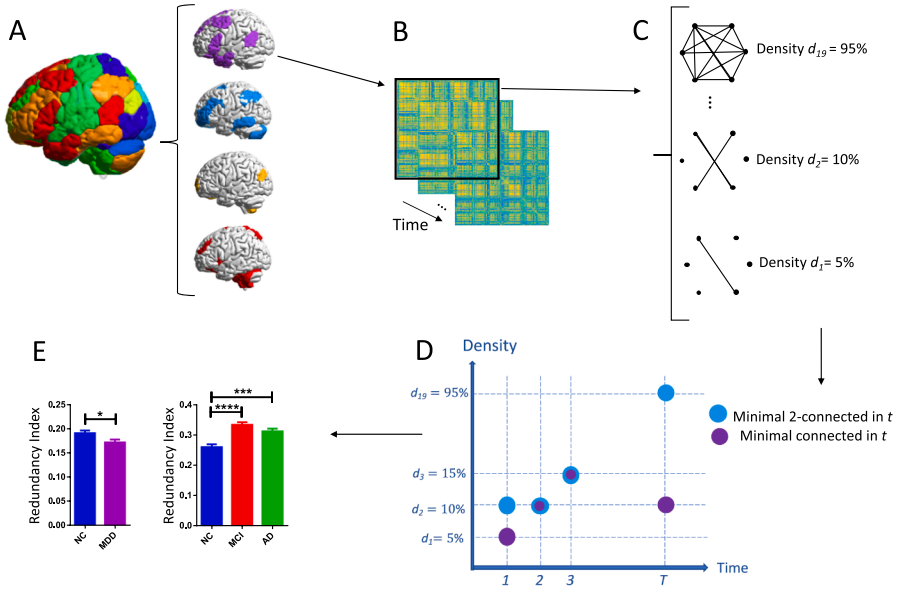

Fig. 3. Schematic framework dynamic redundancy analysis at the subnetwork level. The procedure includes (A) extracting FC subnetworks, (B) sliding window-based dynamic FC analysis, (C) constructing binary networks with different density levels in each sliding window, (D) calculating redundancy index based on a redundancy state vector, and (E) statistical analysis on the redundancy indices. (The figure in Fig. 3E is based on actual data, while the left one shows redundancy index differences in the MF subnetwork between NC and MDD, and the right one shows redundancy index differences in the SUB subnetwork among NC, MCI and AD. (*, **, ***, **** indicate corrected *p*-values (Bonferroni correction) at the intervals of (0.01,0.05], (0.001,0.01], (0.0001,0.001], and (0.00001,0.0001], respectively.)

included). Please note, since the redundancy index was determined by focusing on the minimal connected network at every time window, this study was irrelevant to a specific network density level.

In this study, D = 19 (from 5% to 95% with a step size of 5%), T = 111 for AD study, and T = 151 for MDD study. All the analyses were implemented in MATLAB 2018b (the Mathworks, Inc.), SAGE 8.6 (based on Python 2.7), and SPSS v23 (IBM, Inc.).

2.5. Statistical analysis

Statistical analysis was carried out to compare the redundancy index among different groups (Fig. 3E). We used the Kruskal-Wallis test, a non-parametric version of ANOVA for group comparisons among NC, MCI, and AD groups on each subnetwork and each subnetwork pair ($p < 0.05$, false discovery rate (FDR) corrected). If a significant group difference was detected, then pairwise post-hoc analysis will be conducted with Mann-Whitney U-tests, a non-parametric version of two-sample *t*-test ($p < 0.05$ after Bonferroni correction). As a different analysis, we also conducted Spearman's correlation analysis between each subject's MMSE score and the redundancy index across all the subjects (NC, MCI, and AD) to characterize the possible association between redundancy and cognitive ability in the AD continuum. In the MDD study, we conducted the Mann-Whitney U-tests to detect significant differences in the redundancy indices between NC and MDD groups ($p < 0.05$, FDR corrected). We also conducted Spearman's correlation analysis between the duration of MDD disease and the redundancy index across all the subjects (NC and MDD) to find if there would be any associations between these two metrics.

3. Results

3.1. Group differences in subnetwork's redundancy (the AD study)

We found significant group differences in dynamic redundancy for the default mode and subcortical-cerebellum subnetworks among NC, MCI and AD groups (Table 1, Fig. 4). For subnetwork pairs, we also found group differences in four subnetwork pairs, mostly involving the connections with the subcortical-cerebellum subnetwork and those with the medial frontal subnetwork (Fig. 4C-F). Post-hoc analysis revealed that, in most cases, MCI subjects had elevated redundancy compared to NC, while such an elevation tends to be kept in AD subjects. The only exception was the default mode subnetwork, whose redundancy only decreased in the AD stage compared to NC.

3.2. Association between subnetwork's redundancy and cognitive performance (the AD study)

We found significant correlations between the subnetwork's redundancy index and disease symptoms (MMSE score) across all 147 participants in the AD continuum. They were summarized in Table 2

Table 1
P values from the pairwise comparison with Mann-Withney *U* tests on the significant dynamic redundancy among NC, MCI and AD groups.

	MF	FP	DM	SUB	MF&F	MF&DM	MF& SUB	FP&DM	FP& SUB	DM&SUB
ANOVA	0.359	0.299	**0.03**	**0.000**	**0.002**	0.236	**0.000**	0.574	**0.000**	**0.000**
NC vs. MCI			0.132	**0.000**	**0.001**		**0.000**		**0.000**	**0.000**
AD vs. MCI			0.18	0.103	0.817		0.06		0.164	0.669
NC vs. AD			**0.011**	**0.000**	**0.005**		**0.000**		**0.000**	**0.000**

The *p*-values in **bold** denote significant results after FDR corrections (for three-group comparisons) or after Bonferroni correction (for post-hoc pairwise comparisons). MF: medial frontal subnetwork, FP: frontoparietal subnetwork, DM: default mode subnetwork, SUB: subcortical-cerebellum subnetwork.

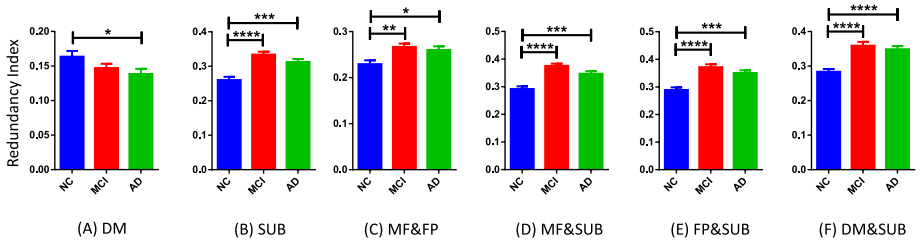

Fig. 4. Group differences in subnetwork's dynamic redundancy among the NC, MCI and AD groups (*, **, ***, **** indicate corrected *p*-values (Bonferroni correction) at the intervals of (0.01,0.05], (0.001,0.01], (0.0001,0.001], and (0.00001,0.0001], respectively). Error bars show standard errors (SE). MF: medial frontal subnetwork, FP: frontoparietal subnetwork, DM: default mode subnetwork, SUB: subcortical-cerebellum subnetwork.

Table 2
Correlations between subnetwork's redundancy index and MMSE across all subjects in the AD study.

	MF	FP	DM	SUB	MF&FP	MF&DM	MF&SUB	FP&DM	FP&SUB	DM&SUB
r	0.75	0.07	0.133	**−0.236**	0.116	−0.177	**−0.251**	0.162	**−0.249**	**−0.307**
p	0.369	0.397	0.109	**0.004**	0.162	0.032	**0.002**	0.05	**0.002**	**0.0001**

Bold values denote significant correlation after FDR corrections ($p < 0.05$). The *r* values indicate Spearman's correlation coefficients. MF: medial frontal subnetwork, FP: frontoparietal subnetwork, DM: default mode subnetwork, SUB: subcortical-cerebellum subnetwork.

(Spearman's correlation, FDR corrected) and the fitted lines were depicted in Fig. 5.

All the results indicate negative correlations between MMSE and the redundancy index. In other words, the redundancy was increased when the symptom was getting worse. By increasing the MMSE, the tendency of redundancy decreases in some of the subnetworks. More importantly, all the significant associations involved either the subcortical-cerebellum subnetwork or the connections with this subnetwork (especially, to the default mode, frontoparietal, and medial frontal subnetworks).

3.3. Group differences in subnetwork's redundancy (the MDD study)

We found significantly decreased subnetwork redundancy (see Fig. 6A) of the medial frontal ($p = 0.016$) and that of the connections between the medial frontal and frontoparietal subnetworks ($p = 0.013$) in the MDD compared to NC after FDR corrections, while other subnetworks and subnetwork pairs did not (Zhi, et al., 2018) show significant changes.

3.4. Correlation between disease duration and subnetwork's redundancy (the MDD study)

Of all the studied subnetworks, we found a significant negative correlation ($r = -0.249$ and $p = 0.044$, uncorrected) between the default mode subnetwork's redundancy index and the disease duration of the MDD subjects (Fig. 6B). As disease duration increased, the redundancy index decreased.

4. Discussions

Graph theory has become a powerful tool in investigating brain network topological changes in diseased populations, including AD (Farahani, et al., 2019) and also MDD (Zhi, et al., 2018). This paper investigated connectedness, a graph theory metric that measures reachability from any node to any other node in the network. If pairs of nodes are reachable through more than one independent path, then the increased reachability makes the network 2-connected, and making the network redundant. The redundancy of the functional brain network

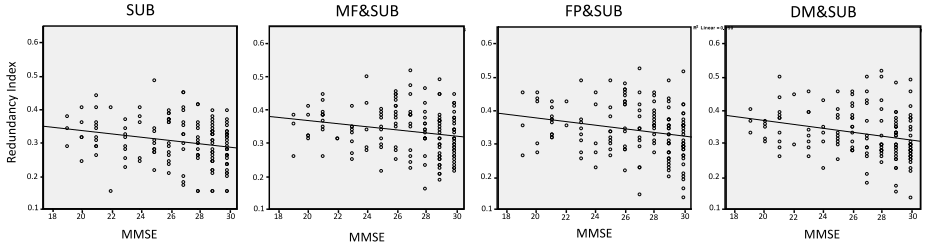

Fig. 5. Scatter plots and the fitted line between MMSE and redundancy indices in AD progression. FP: frontoparietal subnetwork, DM: default mode subnetwork, SUB: subcortical-cerebellum subnetwork.

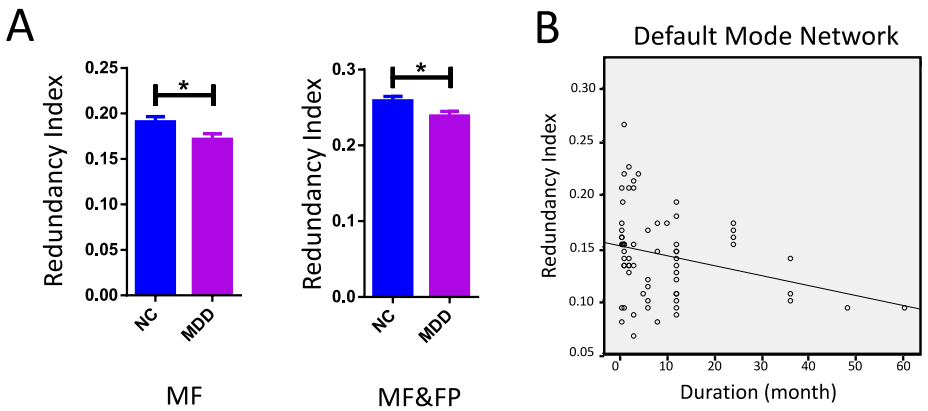

Fig. 6. (A) Comparisons of the subnetwork's redundancy indices between NC and MDD (* indicates $p < 0.05$, FDR corrected). Error bars show standard errors (SE). MF: medial frontal subnetwork, FP: frontoparietal subnetwork. (B) Results of correlation analysis in MDD.

could increase the robustness of the network from attacks to any place in the network. Different disease statuses could alter the redundancy of brain networks, making such an index a suitable measurement of disease perturbation to the brain network. Under such a hypothesis, we have introduced this type of graph theory metrics into brain network research (Ghanbari, et al., 2020, Ghanbari, et al., 2021) and in this paper, tested its feasibility in characterizing different brain subnetworks for different brain diseases. This metric has distinctive features compared to the previous brain network studies. Previous studies may use connectedness as a prerequisite to quantify other network attributes (Rubinov & Sporns, 2010). They did not directly study connectedness and redundancy and its dynamics in diseased conditions. Importantly, we focused on characterizing truly redundant paths (those sharing no nodes) and redundancy for *all* node pairs in the network. The result showed the effectiveness and sensitivity of our method in disease studies.

Despite the novelty of the method, in this paper, we mainly focused on detecting which brain subnetwork(s) had altered dynamic redundancy due to two different diseases (AD and MDD), because it had been shown that complex psychiatric and neurological disorders were characterized by structural and functional abnormalities in a few brain subnetworks (Menon, 2011). With this considered, in the current study, we did not investigate the *global* redundancy of the entire network but the redundancy of the specific brain subnetworks.

We first applied the method to characterize group differences among groups at different AD progression stages. The gradual reduction in the redundancy of the default mode network found along the AD continuum (Fig. 4A) was consistent with the previous findings with other methods (Xue et al., 2019), (Grieder, et al., 2018). This finding indicates that the AD pathology may target the default mode network. However, we did not find significant reductions in the MCI stage, possibly due to a good resilience of the default mode network, which makes its robustness last rather long and finally collapse in the AD stage. This is also different from our previous study characterizing the redundancy of the entire brain network, where the MCI shows elevated redundancy compared to NC and AD. One possible explanation for such a difference is that the default mode subnetwork is losing its redundancy, but other subnetworks are gaining redundancy to compensate for it. This could make the entire network of MCI have increased redundancy. This study, however, further revealed the subnetwork-level changes under the AD pathological attacks.

The generally increased subnetwork redundancy in MCI, as one of the major findings in the current study, is consistent with our previous finding of the elevated whole-brain network redundancy in MCI, arguably caused by the compensatory effect to the AD pathological attack in the early stage. We note that the most involved subnetwork was the subcortical-cerebellum subnetwork. The redundancy of this subnetwork (Fig. 4B) and that of the inter-subnetwork connections with this subnetwork (Fig. 4D-F) were increased in MCI compared to NC. The function of this subnetwork is complex, including memory. Many AD pathology-related regions, such as the hippocampus, are included in this subnetwork. Due to its fundamental role in AD pathology, the connections within this subnetwork could be less efficient; to maintain cognitive ability in the presence of AD-related neurodegeneration, the elevated redundancy in this subnetwork could be the key in the MCI stage. Besides, we found that all three major "high-order" subnetworks (medial frontal, frontoparietal and default mode subnetworks) tended to have more redundant connections to the subcortical-cerebellum regions (Fig. 4D-F). This may further support the "compensatory hypothesis", as the additional paths to these three high-order subnetworks could prevent a significant drop in the cognitive performance. In addition, we found that such elevations were still maintained in the AD stage, whereas it was not the case in our previous whole-brain analysis. This could be due to the smaller scale of the brain network we were currently focused on. Of note, the elevated redundancy was also observed between the medial frontal and the frontoparietal subnetworks, showing the backup paths could also help to maintain the interactions between the high-order subnetworks for high-level cognitive functions in MCI.

Another main finding of the redundancy changes in the AD study lies in the association between disease symptom (general cognitive ability, as measured by MMSE) and the redundancy index in the AD continuum, related to the correlation of the redundancy index and MMSE of the subjects in the AD progression study. By Fig. 5, this negative correlation was consistent with our group comparison results, indicating increased redundancy when the symptom was getting worsened. This result indicates that our proposed subnetwork redundancy index could be sensitive to an early sign of AD, which is better than the whole-brain redundancy. Such a protective mechanism through enhanced redundancy could be used to prevent or delay AD progression in future studies.

We also demonstrated the effectiveness of our method in the MDD study and found that the redundancy loss in the medial frontal subnetwork, as well as the connections between the medial frontal and frontoparietal subnetworks, could be associated with MDD. Previously, in MDD studies, disrupted brain network's efficiency properties have been demonstrated (Zhang, et al., 2011). The most targeted subnetworks in the MDD studies include three high-order networks, i.e., the medial frontal, frontoparietal, and default mode network, as well as their interactions (Kaiser, et al., 2015). Our redundancy index also indicated disrupted medial frontal subnetwork, as well as the medial frontal-frontoparietal interactions (Fig. 6A). Specifically, MDD's subnetwork seemed to have less tendency to be redundant in these subnetworks. The MDD's pathology or neuromechanics have mainly been related to aberrant neurotransmitters in the subcortical (e.g., the striatum) regions (Kumar, et al., 2014), but the disrupted cortical (especially the prefrontal cortex (Zuo, et al., 2018)) to subcortical connections have been

often reported, which involved the medial frontal subnetwork. The functions of this subnetwork also include emotion processes and social behaviors (Waugh, et al., 2014), while the functions of the frontoparietal network mainly include executive control (Veldsman, et al., 2020). The loss of the medial frontal network's redundancy, as well as the connectivity redundancy between this subnetwork and the frontoparietal network could be the cause of uncontrolled depressive thoughts and negative affections (Ross & Rush, 1981). Besides, from the default mode network where the redundancy level was not significantly affected, we found that increased disease duration could reduce this network's redundancy. Taken together, this new redundancy index could also help better understand mental disorders.

We think that the number of redundant connections would decrease after the emerging of major depressive disorder due to the disturbance of the disease. This happened to two subnetworks, MF and MF&FP (Fig. 6A), both are believed to be related to the symptom of depression (Kaiser, et al., 2015). On the contrary, the course of AD could be rather long, with many years developing until MCI and many more years to dementia (Petersen, et al., 2018). With AD pathological changes in the brain, the symptoms could still be invisible or relatively mild. It is hypothesized that the brains of MCI patients may have adequate time to react to the AD pathological attacks by developing compensatory alterations such as increased FC (Skouras, et al., 2019), which may result in elevated connectivity redundancy, possibly by enhancement of weak FC links or redistribution of FC links, to be able to maintain overall connectedness even with the attacks of AD. The decrease of the redundant connections from MCI to AD (Fig. 4) further favors such a hypothesis. That is, with AD progression, the compensation could not make the entire brain network sufficiently work properly, possibly to due the attack to the redundant connections, which eventually causes collapse and dementia.

Our study has several limitations. First, since our method is based on the frequency of redundancy through the time, this technique can only be applied to dynamic FC in the networks, not the static ones; future works could be carried out based on static FC network or even the structural networks. Second, mediation analysis is considered a very promising method in the study of abnormal aging by treating brain network-derived redundancy (robustness) as a certain protective mechanism that could lead to individual differences in the disease progression, which deserves more studies in the future. Third, we applied our methods just to two kinds of diseases, which should be extended to other disorders in the future. Fourth, our redundancy metric is based on the 2-connected graph; a new metric can be defined based on other redundancy measurements, such as 3-connectedness. Fifth, our method is based on binary graphs; how to measure redundancy of a weighted graph needs further study. Finally, instead of conducting group-level statistical analysis, it would be attractive to apply machine learning algorithms on various redundancy features in the future.

5. Conclusions

In this study, we carried out a subnetwork-level redundancy analysis that characterized dynamic redundancy within and between specific subnetworks using resting-state fMRI from two disease cohorts (AD and MDD). We revealed the effectiveness and sensitivity of our subnetwork redundancy index in the brain disease studies. Redundancy, as one of the key metrics in the field of graph theoretic analysis, could be a promising method in the brain network studies.

6. Funding statement

M.G. was supported by the National Institutes of Health grants (EB022880, AG041721). W.J. was supported by the National Institutes of Health grants (MH110274, EB006733) and a grant from Nestec S.A. (RDNN201704). P.-T.Y. was supported by the National Institutes of Health grant (EB022880 and EB006733).

7. Data availability statement

The data and codes are available from the corresponding authors upon reasonable request.

8. Ethics approval

The experiments and data collection were approved by the local ethics committees, as mentioned in the ADNI data sharing website http://adni.loni.usc.edu. For MDD study, all participants provided written informed consent and the study was approved by the local ethics committee.

9. Consent to participate

Data used from ADNI is publicly available, so this is not applicable. The MDD data are not publicly available due to privacy or ethical restrictions.

Declaration of Competing Interest

The authors declare that they have no known competing financial interests or personal relationships that could have appeared to influence the work reported in this paper.

References

Achard, S., Salvador, R., Whitcher, B., et al., 2006. A resilient, low-frequency, small-world human brain functional network with highly connected association cortical hubs. J. Neurosci. 26 (1), 63–72.
American Psychiatric Association, 2013. Diagnostic and statistical manual of mental disorders: DSM-5, 5th ed. American Psychiat- ric Publishing Inc., Arlington, VA.
Bludau, S., Bzdok, D., Gruber, O., et al., 2016. Medial prefrontal aberrations in major depressive disorder revealed by cytoarchitectonically informed voxel-based morphometry. American J. Psychiatry. 173 (3), 291–298.
Chang, C., Glover, G.H., 2010. Time–frequency dynamics of resting-state brain connectivity measured with fMRI. Neuroimage 50 (1), 81–98.
Chen, X., Zhang, H., Zhang, L., et al., 2017. Extraction of dynamic functional connectivity from brain grey matter and white matter for MCI classification. Hum. Brain Mapp. 38 (10), 5019–5034.
Corson, F., 2010. Fluctuations and redundancy in optimal transport networks. Phys. Rev. Lett. 104 (4), 048703.
Cox, R.W., 1996. AFNI: software for analysis and visualization of functional magnetic resonance neuroimages. Comput. Biomed. Res. 29 (3), 162–173.
Cui, X., Xiang, J., Guo, H., et al., 2018. Classification of Alzheimer's disease, mild cognitive impairment, and normal controls with subnetwork selection and graph Kernel principal component analysis based on minimum spanning tree brain functional network. Front. Comput. Neurosci. 12, 31.
Di Lanzo, C., Marzetti, L., Zappasodi, F., et al. 2012. Redundancy as a graph-based index of frequency specific MEG functional connectivity. Computational and mathematical methods in medicine.
Fallani, F.D., Rodrigues, F.A., da Fontoura Costa, L., et al., 2011. Multiple pathways analysis of brain functional networks from EEG signals: an application to real data. Brain Topogr. 23 (4), 344–354.
Farahani, F.V., Karwowski, W., Lighthall, N.R., 2019. Application of graph theory for identifying connectivity patterns in human brain networks: a systematic review. Front. in Neurosci. 13, 585.
Ghanbari, M., Hsu, L.-M., Zhou, Z., et al. 2020. A New Metric for Characterizing Dynamic Redundancy of Dense Brain Chronnectome and Its Application to Early Detection of Alzheimer's Disease. In International Conference on Medical Image Comput. and Computer-Assisted Intervention (pp. 3-12). Springer, Cham.
Ghanbari, M., Zhou, Z., Hsu, L.-M., et al. 2021, Altered Connectedness of the Brain Chronnectome During the Progression to Alzheimer's Disease, Neuroinformatics, https://doi.org/10.1007/s12021-021-09554-3.
Grieder, M., Wang, D.J.J., Dierks, T., Wahlund, L.-O., Jann, K., 2018. Default mode network complexity and cognitive decline in mild Alzheimer's disease. Front. in Neurosci. 12 https://doi.org/10.3389/fnins.2018.0077010.3389/fnins.2018.00770.s00110.3389/fnins.2018.00770.s002.
Hamilton, M., 1967. Development of a rating scale for primary depressive illness. British Journal of Social and Clinical Psychology 6, 278–296.
Härkegård, O., Glad, S.T., 2005. Resolving actuator redundancy—optimal control vs. control allocation. Automatica. 41 (1), 137–144.
Joyce, K.E., Hayasaka, S., Laurienti, P.J., Achard, S., 2013. The human functional brain network demonstrates structural and dynamical resilience to targeted attack. PLoS Comput Biol. 9 (1), e1002885.
Kaiser, R.H., Andrews-Hanna, J.R., Wager, T.D., Pizzagalli, D.A., 2015. Large-scale network dysfunction in major depressive disorder: a meta-analysis of resting-state

functional connectivity. JAMA psychiatry. 72 (6), 603. https://doi.org/10.1001/jamapsychiatry.2015.0071.
Kumar, A., Yang, S., Ajilore, O., et al., 2014. Subcortical biophysical abnormalities in patients with mood disorders. Mol. Psychiatry 19 (6), 710–716.
Leistritz, L., Weiss, T., Bär, K.J., et al., 2013. Network redundancy analysis of effective brain networks; a comparison of healthy controls and patients with major depression. PLoS ONE 8 (4), e60956.
Li, G., Liu, Y., Zheng, Y., et al., 2020. Large-scale dynamic causal modeling of major depressive disorder based on resting-state functional magnetic resonance imaging. Hum. brain map. 41 (4), 865–881.
Liu, J., Li, M., Pan, Y.i., Lan, W., Zheng, R., Wu, F.-X., Wang, J., 2017. Complex brain network analysis and its applications to brain disorders: a survey. Complexity 2017, 1–27.
Marusak, H.A., Calhoun, V.D., Brown, S., et al., 2017. Dynamic functional connectivity of neurocognitive networks in children. Hum. Brain Mapp. 38 (1), 97–108.
Menon, V., 2011. Large-scale brain networks and psychopathology: a unifying triple network model. Trends in Cognitive. Sci. 15 (10), 483–506.
Newman, M.E., 2006. Modularity and community structure in networks. Proc. Natl. Acad. Sci. 103 (23), 8577–8582.
Petersen, R.C., Lopez, O., Armstrong, M.J., Getchius, T.S.D., Ganguli, M., Gloss, D., Gronseth, G.S., Marson, D., Pringsheim, T., Day, G.S., Sager, M., Stevens, J., Rae-Grant, A., 2018. Practice guideline update summary: Mild cognitive impairment: Report of the Guideline Development, Dissemination, and Implementation Subcommittee of the American Academy of Neurology. Neurology 90 (3), 126–135.
Ravasz, E., Barabási, A.L. 2003. Hierarchical organization in complex networks. Physical review E. 14, 67(2), 026112..
Ross, E.D., Rush, A.J., 1981. Diagnosis and neuroanatomical correlates of depression in brain-damaged patients: implications for a neurology of depression. Arch. Gen. Psychiatry 38 (12), 1344–1354.
Rubinov, M., Sporns, O., 2010. Complex network measures of brain connectivity: uses and interpretations. Neuroimage. 52 (3), 1059–1069.
Sampath, D., Sathyanesan, M., Newton, S.S., 2017. Cognitive dysfunction in major depression and Alzheimer's disease is associated with hippocampal–prefrontal cortex dysconnectivity. Neuropsychiatr. Dis. Treat. 13, 1509.
Saunders, J., Aasland, O., Babor, T.F., et al., 1993. Development of the alcohol use disorders identification test (AUDIT): WHO collaborative project on early detection of persons with harmful alcohol consumption—II. Addiction 88, 791–804.
Shen, X., Tokoglu, F., Papademetris, X., et al., 2013. Groupwise whole-brain parcellation from resting-state fMRI data for network node identification. Neuroimage. 82, 403–415.
Sierksma, A.S., van den Hove, D.L., Steinbusch, H.W., et al., 2010. Major depression, cognitive dysfunction and Alzheimer's disease: is there a link? Eur. J. Pharmacol. 626 (1), 72–82.
Skouras, S., Falcon, C., Tucholka, A., et al., 2019. Mechanisms of functional compensation, delineated by eigenvector centrality mapping, across the pathophysiological continuum of Alzheimer's disease. NeuroImage: Clinical 22, 101777.
Smith, S.M., Fox, P.T., Miller, K.L., et al., 2009. Correspondence of the brain's functional architecture during activation and rest. Proc. Natl. Acad. Sci. 106 (31), 13040–13045.
Sporns, O., 2013. Structure and function of complex brain networks. Dialogu. in Clin. Neurosc. 15 (3), 247.
Veldsman, M., Tai, X.Y., Nichols, T., et al., 2020. Cerebrovascular risk factors impact frontoparietal network integrity and executive function in healthy ageing. Nature communications.11(1), 1.
Waugh, C.E., Lemus, M.G., Gotlib, I.H., 2014. The role of the medial frontal cortex in the maintenance of emotional states. Social Cognitive and Affective Neurosci. 9 (12), 2001–2009.
Xuan, H., Gan, C., Li, W., et al., 2017. Altered network efficiency of functional brain networks in patients with breast cancer after chemotherapy. Oncotarget. 8 (62), 105648.
Xue, C., Yuan, B., Yue, Y., et al., 2019. Distinct disruptive patterns of default mode subnetwork connectivity across the spectrum of preclinical Alzheimer's disease. Frontiers in aging Neurosci. 11, 307.
Yan, C., Zang, Y., 2010. DPARSF: a MATLAB toolbox for" pipeline" data analysis of resting-state fMRI. Frontiers in Systems Neurosci. 4, 13.
Yan, C.G., Chen, X., Li, L., et al., 2019. Reduced default mode network functional connectivity in patients with recurrent major depressive disorder. Proceedings of the National Academy of Scien. 116 (18), 9078–9083.
Yoo, S.W., Han, C.E., Shin, J.S., et al., 2015. A network flow-based analysis of cognitive reserve in normal ageing and Alzheimer's disease. Sci. Rep. 5 (1), 1–4.
Zhang, J., Wang, J., Wu, Q., et al., 2011. Disrupted brain connectivity networks in drug-naive, first-episode major depressive disorder. Biol. Psychiatry 70 (4), 334–342.
Zhi, D., Ma, X., Lv, L., et al., 2018. Abnormal dynamic functional network connectivity and graph theoretical analysis in major depressive disorder. In: In2018 40th Annual International Conference of the IEEE Engineering in Medicine and Biology Society (EMBC), pp. 558–561.
Zuo, Z., Ran, S., Wang, Y., et al., 2018. Altered structural covariance among the dorsolateral prefrontal cortex and amygdala in treatment-naive patients with major depressive disorder. Front. in psychiatry. 9, 323.